

The high temperature expansion of the classical XYZ chain

E.V. Corrêa Silva,¹ Onofre Rojas,² James E.F. Skea,³ S.M. de Souza,⁴ and M.T. Thomaz^{5,*}

¹*Departamento de Matemática e Computação, Faculdade de Tecnologia,
Universidade do Estado do Rio de Janeiro. Estrada Resende-Riachuelo,
s/nº, Morada da Colina, CEP 27523-000, Resende-RJ, Brazil*

²*Departamento de Ciências Exatas, Universidade Federal de Lavras,
Caixa Postal 3037, CEP 37200-000, Lavras-MG, Brazil*

³*Instituto de Física, Universidade do Estado do Rio de Janeiro,
R. São Francisco Xavier nº 524, Bloco B, CEP- 20559-900, Rio de Janeiro -RJ, Brazil*

⁴*Departamento de Ciências Exatas, Universidade Federal de Lavras,
Caixa Postal 37, CEP 37200-000, Lavras-MG, Brazil*

⁵*Instituto de Física, Universidade Federal Fluminense,
Av. Gal. Milton Tavares de Souza s/nº, CEP 24210-340, Niterói-RJ, Brazil*

(Dated: October 12, 2018)

We present the β -expansion of the Helmholtz free energy of the classical XYZ model, with a single-ion anisotropy term and in the presence of an external magnetic field, up to order β^{12} . We compare our results to the numerical solution of Joyce's [Phys. Rev. Lett. **19**, 581 (1967)] expression for the thermodynamics of the XXZ classical model, with neither single-ion anisotropy term nor external magnetic field. This comparison shows that the derived analytical expansion is valid for intermediate temperatures such as $kT/J_x \approx 0.5$. We show that the specific heat and magnetic susceptibility of the spin-2 antiferromagnetic chain can be approximated by their respective classical results, up to $kT/J \approx 0.8$, within an error of 2.5%. In the absence of an external magnetic field, the ferromagnetic and antiferromagnetic chains have the same classical Helmholtz free energy. We show how this two types of media react to the presence of an external magnetic field.

1. INTRODUCTION

The classical limit of quantum spin chains has attracted attention since this class of models was proposed to describe the magnetic interactions of one-dimensional models. In 1964 Fisher[1] calculated the analytical expression of the Helmholtz free energy (HFE) of the XXX chain in the presence of an external magnetic field. Some years later, Joyce[2] included in that model an anisotropy term of interaction between the z components of neighbouring spins, and obtained its exact HFE for a vanishing external magnetic field. Since then the thermodynamics of the classical XXX chain, in the presence of in-plane or transverse magnetic field has been studied at very low temperatures (limit of long wavelength) and the mapping of this classical spin chain into the Sine-Gordon model[3] has permitted one to obtain analytical expressions for some thermodynamical functions in this region of temperature. On the other hand, the classical XXZ chain in the presence of an external magnetic field in the z direction has also been studied numerically[4].

Recently we obtained the high temperature expansion (HTE) of the HFE of the quantum spin- S XYZ chain[5], with a single-ion anisotropy term and in the presence of an external magnetic field, up to order β^5 . (Here we have $\beta = \frac{1}{kT}$, where k is the Boltzmann's constant, T is the temperature in Kelvin.) The HFE of the classical model is obtained from Ref. [5] by taking the limit $S \rightarrow \infty$,

where S is the spin value ($S = 1/2, 1, 3/2, 2, \dots, \infty$). The calculation of this thermodynamical function of the quantum model was done by using the cumulant series for the one-dimensional models presented in Ref. [6]. This approach can also be applied to classical periodic chain models with nearest-neighbor interactions. To the best of our knowledge, analytical expressions of the HFE for intermediate and high temperature regions of the classical XYZ model are currently unknown.

In Ref. [5], we showed that certain thermodynamical functions like the magnetization and magnetic susceptibility per site of the quantum XYZ chain can be well approximated, in the intermediate and high temperature regions, by their classical results for $S \geq 3/2$. The absence of results for the quantum XYZ chain for $S > 1/2$, makes the knowledge of the classical model very interesting in the region of $kT \gtrsim J_x$, where J_x is the coupling constant between the closest spins along the x direction. Even for other thermodynamical functions, like the specific heat per site, the classical models give results with the correct order of magnitude for those regions of temperature. Nowadays the possibility of designing different materials with suitable properties turn the analytical expressions of the classical thermodynamical functions to be very helpful.

In Ref. [5] we calculated the β -expansion of the HFE of the quantum and classical XYZ model, with single-ion anisotropy term and in the presence of an external magnetic field, up to order β^5 . When applying the method of Ref. [6] directly to the classical model we have the advantage of calculating traces of c -numbers, thus diminishing the number of terms to be evaluated. Here is the first

*Corresponding author: mtt@if.uff.br

time that this method is being applied directly to a classical periodic chain with first-neighbour interactions.

In section 2, we present the Hamiltonian that describes the classical XYZ chain with unitary spin ($|\vec{s}_i| = 1$) at the i -th site. In this model we take into account the presence of a single-ion anisotropy term and an external magnetic field along the z direction. In section 3, we present the results of Ref.[6] when applied directly to the classical XYZ chain; a rule is obtained that allows, in the present case, optimization of the algebraic calculations of the HFE. In section 4, we compare Joyce's solution[2] with our results for the particular case of a classical XXZ chain ($J_x = J_y$) without the single-ion anisotropy term ($D = 0$) and in the absence of an external magnetic field ($h = 0$), for intermediate and high temperatures. Joyce's solution of the classical XXZ chain allows one to obtain the behaviour of the specific heat per site at low temperatures, and then apply Padé's method to extend the validity of the HTE to lower temperatures. In section 5 we study some thermodynamical functions of the classical XYZ chain in the presence of an external magnetic field. Finally, in section 6 we present a summary of our results.

In appendix A, we present some useful integral results. As an example of our HTE of the HFE of the classical XYZ chain, we present in appendix B its expansion up to order β^6 in the absence of an external magnetic field. Its complete expansion, up to order β^{12} , is quite lengthy and can be obtained under request to the authors.

2. THE CLASSICAL XYZ CHAIN WITH UNITARY SPIN

The classical version of the hamiltonian of the anisotropic XYZ chain with unitary spin- S , as shown in Eq.(2) of Ref. [5], is

$$\mathbb{H} = \sum_{i=1}^N \mathbf{H}_{i,i+1} = \sum_{i=1}^N \{J_x s_i^x s_{i+1}^x + J_y s_i^y s_{i+1}^y + J_z s_i^z s_{i+1}^z - h s_i^z + D(s_i^z)^2\}, \quad (1)$$

where

$$\begin{aligned} s_i^x &= \sin(\theta_i) \cos(\phi_i), & s_i^y &= \sin(\theta_i) \sin(\phi_i), \\ s_i^z &= \cos(\theta_i); \end{aligned} \quad (2)$$

θ_i and ϕ_i are the polar and azimuthal angles, respectively, of the classical spin \vec{s}_i ; N is the number of sites in the periodic chain; h is the external magnetic field along the z -axis and D is the single-ion anisotropy parameter. The constants J_x , J_y and J_z give the strength of first-neighbour interactions between the components of the spins. From (1) and (2), we define the function \mathcal{H} , so that

$$\mathbb{H} = \sum_{i=1}^N \mathcal{H}(\theta_i, \phi_i, \theta_{i+1}, \phi_{i+1}). \quad (3)$$

3. THE METHOD OF CUMMULANT SERIES APPLIED TO CLASSICAL CHAINS

In Ref. [7] we presented a survey of the cumulant series method and its application to one-dimensional periodic *quantum* chain models with first-neighbour interactions. Here, we discuss the application of this method to any *classical* one-dimensional chain model subject to periodic boundary conditions, spatial translation invariance, and nearest-neighbor interactions. Following Ref. [6], we obtain the analytical expressions for the HTE of the HFE in the thermodynamical limit of such models, which can be written as the β -expansion

$$\mathcal{W}(\beta) = -\frac{1}{\beta} [\ln(\text{tr}_i(\mathbf{1}_i)) + \ln(1 + \xi(\beta))], \quad (4)$$

where $\text{tr}_i(\mathbf{1}_i)$ equals the dimension of the classical Hilbert space of the i -th site,

$$\xi(\beta) = \sum_{n=0}^{\infty} \frac{1}{(n+1)!} \frac{\partial^n}{\partial \lambda^n} (\varphi(\lambda)^{n+1}) \Big|_{\lambda=1} \quad (5)$$

and the auxiliary function $\varphi(\beta)$ is given by

$$\varphi(\lambda) = \sum_{m=1}^{\infty} \sum_{n=m}^{\infty} \frac{(-\beta)^n}{\lambda^m} H_{1,m}^{(n)}. \quad (6)$$

The functions $H_{1,m}^{(n)}$ correspond to the “connected” strings with n operators $\mathbf{H}_{i,i+1}$ (in the present case, see Eq. (1)) so that m of them are distinct, that is,

$$H_{1,m}^{(n)} = \sum_{\{n_i\}}^n \left\langle \prod_{i=1}^m \frac{\mathbf{H}_{i,i+1}^{n_i}}{n_i!} \right\rangle. \quad (7)$$

The normalized trace is defined as

$$\langle \mathbf{H}_{i_1,i_1+1} \dots \mathbf{H}_{i_m,i_m+1} \rangle \equiv \frac{\text{tr}_{i_1, \dots, i_m+1} (\mathbf{H}_{i_1,i_1+1} \dots \mathbf{H}_{i_m,i_m+1})}{\text{tr}_{i_1}(\mathbf{1}_{i_1}) \dots \text{tr}_{i_m+1}(\mathbf{1}_{i_m+1})}, \quad (8)$$

where the indices i_1, \dots, i_m can be equal or distinct. The notation $\text{tr}_{i_1, \dots, i_m+1}$ stands for the trace over the degrees of freedom of $m+1$ distinct sites in the set: $\{i_1, \dots, i_m+1\}$, with $m \leq n$. In addition, tr_{i_k} represents the trace over the degrees of freedom of the i_k -th site and $\mathbf{1}_{i_k}$ is its identity operator.

Eq.(7) differs from its quantum version on showing a normalized trace, rather than a g -trace: in the classical case, all $\mathbf{H}_{i,i+1}$ are commuting functions. This property greatly simplifies all calculations (see Appendix A). The notation $\sum_{\{n_i\}}^n$ stands for the restriction $\sum_{i=1}^m n_i = n$ and

$n_i \neq 0$ for $i = 1, 2, \dots, m$. The index m satisfies the condition $1 \leq m \leq n$. Equations (4) to (7) are valid for any classical one-dimensional chain model subject to periodic boundary conditions, spatial translation invariance, and nearest-neighbors interactions. In order to reach higher orders in β in the HTE of the HFE, it is important to optimize the calculation of the normalized traces in Eq. (7). Although the classical model has less terms to be calculated than its quantum version, we still have a large number of integrals to be done for each order in β . For Hamiltonian (1) it is straightforward to verify that, at each site, using the results (A.4) and (A.5) of appendix A, that we only have a non-vanishing normalized trace $\langle (s^x)^l (s^y)^m (s^z)^p \rangle$, if and only if l , m and p are all even.

4. THE β -EXPANSION OF THE HFE OF THE CLASSICAL XYZ CHAIN

From the results of Ref. [5], we can obtain the HTE of the HFE of the classical XYZ model, up to order β^5 , by taking the limit of $S \rightarrow \infty$ in its Eq.(3). By using the results of section 3, we obtain here the HTE of the HFE, \mathcal{W}_{class} , up to order β^{12} , for a non-vanishing external magnetic field h and in the presence of a single-ion anisotropy term in the Hamiltonian (1). The derived expansion is very lengthy and it can be obtained from the authors by request. Although this series has a large number of terms, it can be easily handled by any CAS system (we used **Maple**). In appendix B we present the expansion of the HFE of the classical XYZ chain, with unitary spin (see Hamiltonian (1), in the absence of an external magnetic field ($h = 0$)), up to order β^6 . The resulting expansion (B.1) agrees with the series of this thermodynamical function obtained from eq.(3) of Ref. [5], in the limit $S \rightarrow \infty$.

In this section, we have $J_x = J_y = J$ and $J_z = J\Delta$, for the constants in Hamiltonian (1) for the particular case of the classical XXZ model.

4.1. Comparison of the HTE of the classical XXZ chain with Joyce's solution

Next, we perform some comparisons with known results, to verify the interval of temperature where our HTEs still hold. Joyce[2] obtained the exact solution of the classical XXZ chain, without a single-ion anisotropy term ($D = 0$) and in the absence of an external magnetic field ($h = 0$). In order to check our HTE of the classical model and to verify how it extends our previous results[5], we compare in Figs. 1a and 1b the Joyce's numerical solution for the HFE with our expansions up to orders β^5 and β^{12} . In Figs. 1c and 1d we present the respective percental difference between each of those expansions and the exact Joyce's solution. In Fig. 1a we plot the HFE for $\Delta = \pm 0.5$. At first glance of this graph suggests that the expansion up to β^{12} is poorer

than the expansion up to β^5 . However, a closer look at the interval $kT/J = [0.4, 1]$ (see the detail box) shows that the β^{12} -curve coincides with the exact solution up to $kT/J = 0.53$, whereas the β^5 -curve coincides with it only up to $kT/J = 0.9$. In Fig. 1b, we take $\Delta = \pm 1$ and we see that the expansion up to β^5 coincides with the numerical solution of Joyce's expression up to $kT/J = 0.56$ whereas the series up to β^{12} goes up to $kT/J = 0.39$, which can certainly be considered an intermediate region of temperature.

In Fig. 2 we compare the specific heat per site, $C_{class}(\beta) = -\beta^2 \frac{\partial^2}{\partial \beta^2} (\beta \mathcal{W}_{class}(\beta))$, obtained from Joyce's solution of the classical XXZ chain (with $h = 0$ and $D = 0$) and the HTE up to β^6 (see Ref. [5]) and up to β^{13} . We also include (Figs. 2c and 2d) the respective relative percental difference of these expansions to the exact solution. In Fig. 2a we have $J = 1$ and $\Delta = \pm 0.5$, whereas in Fig. 2b we have $J = 0.5$ and $\Delta = \pm 2$. Again, in both plots we verify that the β^{13} expansion extends to lower temperature the validity of the HTE of the classical model in Refs. [5, 8], as shown in the detail box of Fig. 2c. It is simple to derive from Joyce's solution the correlation function between the x , y and z components of the classical spins of first nearest neighbours. Due to the symmetry in the x and y directions in Hamiltonian (1), for $J_x = J_y$, we have $\langle s_i^x s_{i+1}^x \rangle = \langle s_i^y s_{i+1}^y \rangle$. In Figs. 3 we plot the correlation function $\langle s_i^x s_{i+1}^x \rangle = \frac{\partial \mathcal{W}_{class}}{\partial J_x}$ for $J = 1$ and $\Delta = 0.5$ (Fig. 3a) and for $J = 0.5$ and $\Delta = 2$ (Fig. 3b), derived from the exact result and from our β -expansion (up to order β^{12}) for the HFE of the classical model. From Fig. 3b we see that the β^{12} -curve gives the correct maximum of the function $\langle s_i^x s_{i+1}^x \rangle$ for $J = 0.5$ and $\Delta = 2$.

In Figs. 4 we plot the correlation function $\langle s_i^z s_{i+1}^z \rangle = \frac{\partial \mathcal{W}_{class}}{\partial J_z}$ for the exact result of the classical model and our β -expansion, for the same set of constants J and Δ as in Figs. 3. From Fig. 4a we see that the derived HTE up to β^{12} gives the correct maximum of this thermodynamical function.

One way to extrapolate the results of our high temperature series to higher orders in β is through the Padé approximants (PA), which allows us to combine thermodynamical information from both high and low temperatures. Among the several approaches to Padé approximants[9], here we employ the two-point Padé approximant[10] to extend our β -expansion of the specific heat per site to low temperatures.

From the numerical analysis of Joyce's solution[2] of the specific heat per site at very low temperatures, for $J \neq 1$ and $\Delta \neq 1$, we realize that it has a polynomial behaviour in T . For the range of temperature $T \in [0, 0.1]$, it can be chosen to be of fourth order in T , $C(T) \approx 1 + a_1 T + a_2 T^2 + a_3 T^3 + a_4 T^4$, where the coefficients a_i can be adjusted appropriately by linear regression. In this case, we have 5 known terms in the region of low temperature and 12 known terms in the region of high temperature, resulting in a Padé approximant with 17

terms.

Fig. 5a compares results for the specific heat per site, namely the best PAs and Joyce's exact solution, for $J = 1$ and $\Delta = 0.5$. For these constants, we have: $a_1 = 0.51519$, $a_2 = 1.42213$, $a_3 = -2.10687$ and $a_4 = 62.1676$. Below the graph in 5a, we show the percental deviation of each PA with respect to the numerical result of the exact solution. It turns out that $P_{11,6}$ is the best approximation of the exact result, within a difference of less than 2% for all values of temperature.

Fig. 5b shows a similar comparison, but for the parameters values $J = 0.5$ and $\Delta = 2$. For those constants, we obtain numerically: $a_1 = 0.529029$, $a_2 = 1.63073$, $a_3 = -8.64101$ and $a_4 = 86.746$. In Fig. 5c, we present the percental deviation of each PA to the numerical result of the exact solution. We see that $P_{10,7}$ is the best approximation to the exact result. In the whole interval of temperature, its percental difference to the exact solution is less than 10%. Although Figs. 5a and 5b refer to the same thermodynamical function, each case demands specific PAs for the best fitting.

4.2. The classical model as an approximation to the quantum model.

The classical XYZ chain is a good approximation to the quantum chain, for all values of S ($S = 1/2, 1, 3/2, 2, \dots$), in the high temperature region ($J_x\beta \ll 1$). In Ref. [8] we showed that some thermodynamical functions of the quantum XXZ chain can be well approximated by their classical version for not so high temperatures. This region of temperature, where the classical and quantum models are equivalent, depends on the thermodynamical function and on the spin. The higher the spin of the quantum model, the more involved its numerical solution gets, due to the growing number degrees of freedom. However, as far as the XXZ model is concerned, for $S \geq 2$, the quantum HTE of a given thermodynamical quantity can thus be well approximated to its classical HTE.

Some materials are well described by XXZ models with higher values of spin. For example, the $(\text{C}_{10}\text{H}_8\text{N}_2)\text{MnCl}_3$, described by a $S = 2$ model[11]; and the $(\text{CH}_3)_4\text{NMnCl}_3$, also known as TMMC, described by a $S = 5/2$ model[12, 13]. In Ref. [14], Yamamoto carried out Monte Carlo calculations of the thermodynamics of the $S = 2$ XXZ chain with 96 sites, with $\Delta = 1$, $D = 0$ and $h = 0$. He obtained the temperature dependence of the specific heat per site and the magnetic susceptibility per site for any temperature. Fig. 6a compares the numerical results of Yamamoto [14] for the specific heat per site, for the $S = 2$ antiferromagnetic case, to our β -expansion of the *classical* specific heat per site, up to order β^{13} . Fig. 6b shows the relative percental error between these two curves, which is less than 2.5% up to $kT/J = 0.75$. In Fig. 7a we compare Yamamoto's quantum magnetic susceptibility per site ($\chi = -\frac{\partial^2 \mathcal{W}}{\partial h^2}$) of the

$S = 2$ antiferromagnetic chain[14] to its equivalent classical function obtained from our β -expansion, up to order β^{12} . In the same token, Fig. 7b shows their percental difference, which is smaller than 2.5% up to $kT/J \sim 0.8$.

In Ref. [8] we verified that the higher the spin, the closer quantum and classical thermodynamical functions get. The curves, for a given thermodynamical function of the quantum models, do not cross for different values of spin. Although we do not have a numerical study of the thermodynamics of the antiferromagnetic chain with $S = 5/2$, we can affirm that its specific heat and magnetic susceptibility per site, for kT/J up to 0.8, differs from the classical result in less than 2.5%. This also applies to the TMMC[15], since its anisotropy in the z directions is small, namely $\Delta = 0.016$.

5. THE THERMODYNAMICAL FUNCTIONS OF THE CLASSICAL XYZ CHAIN

From expression (B.1) of Appendix B, we verify that the HFE of the classical XYZ chain in the absence of an external magnetic field ($h = 0$), is an even function of the constants J_x , J_y and J_z , so that this function is the same for classical ferromagnetic and antiferromagnetic materials with the same single-ion anisotropy D -term. As a consequence of this property, we have that some thermodynamical functions have well defined parity under the transformation $(J_x, J_y, J_z) \rightarrow (-J_x, -J_y, -J_z)$: the specific heat, $\langle (s_i^z)^2 \rangle$, the entropy and the mean energy are even functions, whereas the first-neighbor correlation functions, $\langle s_i^x s_{i+1}^x \rangle$, $\langle s_i^y s_{i+1}^y \rangle$ and $\langle s_i^z s_{i+1}^z \rangle$ are odd functions. None of the quantum versions of the above mentioned functions have defined parity for $h = 0$ [5].

Figs. 8 show how each type of medium responds to the presence of an external magnetic field. We use the fact that the mean energy per site, $\langle \mathcal{E} \rangle = \frac{\partial(\beta \mathcal{W}_{class})}{\partial \beta}$, is the same for both ferromagnetic and antiferromagnetic media at $h = 0$. Fig. 8a shows the curve of the mean energy as a function of $J_x\beta$, for $J_y/J_x = 1/3$, $J_z/J_x = \pm 2/3$ and $D/J_x = -0.6$, at $h = 0$.

Fig. 8b shows, for the ferromagnetic ($J_z/J_x = -2/3$) and antiferromagnetic ($J_z/J_x = 2/3$) cases, the difference of the mean energy per site with and without external magnetic field (cf. Fig. 8b, $\Delta \mathcal{E} = \langle \mathcal{E} \rangle|_h - \langle \mathcal{E} \rangle|_{h=0}$), plotted as a function of h/J_x , for $J_x\beta = 0.5$ and $J_x\beta = 1$. Fig. 8c quantifies this difference, showing the corresponding percental differences ($\Delta \mathcal{E}(\%) = \frac{\langle \mathcal{E} \rangle|_h - \langle \mathcal{E} \rangle|_{h=0}}{\langle \mathcal{E} \rangle|_{h=0}} \times 100\%$).

The behavior of the mean square of the z -component of each spin in the chain at $h = 0$ as a function of $J_x\beta$, $\langle (s_i^z)^2 \rangle = \frac{\partial \mathcal{W}_{class}}{\partial D}$, can be seen in Fig. 9a. The reaction of the ferromagnetic and antiferromagnetic media to the presence of an external magnetic field, $\langle (s_i^z)^2 \rangle - \langle (s_i^z)^2 \rangle|_{h=0}$, can be seen in Fig. 9b, as a function of h/J_x at $J_x\beta = 0.5$ and $J_x\beta = 1$. For both graphs, we take the same set of values for J_y/J_x , J_z/J_x and D/J_x as that of Fig. 8 for the ferromagnetic and antiferromagnetic

media. Fig. 9c is similar to Fig. 9b, showing the corresponding percental difference with respect to $\langle (s_i^z)^2 \rangle|_{h=0}$.

In Fig. 10 we compare the magnetization per site, $M_{class} = -\frac{\partial \mathcal{W}_{class}}{\partial h}$, at $J_x\beta = 0.8$, for the ferromagnetic case (with $J_y/J_x = 1/3$, $J_z/J_x = -2/3$, $D/J_x = -0.6$) and the antiferromagnetic case (with $J_y/J_x = 1/3$, $J_z/J_x = 2/3$, $D/J_x = -0.6$). For these same cases, in Fig. 11 we compare the classic magnetic susceptibility per site at $h/J_x = 0.35$.

Since we are working with unitary classical spins ($|\vec{s}_i| = 1$), we define $\langle \cos \theta_i \rangle \equiv \langle \vec{s}_i \cdot \vec{s}_{i+1} \rangle$, where θ_i is the angle between the i -th and $(i+1)$ -th spins in the chain. In Fig. 12a we plot the function $\langle \cos \theta_i \rangle \equiv \left(\frac{\partial}{\partial J_x} + \frac{\partial}{\partial J_y} + \frac{\partial}{\partial J_z} \right) \mathcal{W}_{class}$ for the antiferromagnetic case (with $J_y/J_x = 1/3$, $J_z/J_x = 2/3$, $D/J_x = -0.6$), whereas in Fig. 12b we plot $\langle \cos \theta_i \rangle$ for the ferromagnetic case (with $J_y/J_x = 1/3$, $J_z/J_x = -2/3$, $D/J_x = -0.6$), both at $h/J_x = 0.35$. From Fig. 12b we see that at $J_x\beta = 0.9$, on the average, neighboring spins are orthogonal to each other. For these cases, we also plot in Fig. 13 the correlation function $\langle s_i^z s_{i+1}^z \rangle$.

Within the range of the independent variable (h/J_x) shown in Fig. 10, the HTE of the magnetization M is almost equal to its exact solution. This range has been determined so that the HTEs of leading orders β^{11} and β^{12} differs by 0.1% therein. A similar thought guided the determination of the ranges of $J_x\beta$ in Figs. 11 and 13, regarding the magnetic susceptibility χ and correlation function $\langle s_i^z s_{i+1}^z \rangle$, respectively.

6. CONCLUSIONS

The method developed in Ref. [6] can be equally applied to both quantum and classical chains with first-neighbor interactions, spatial periodic boundary conditions and translational invariance. In Ref. [5] we calculated the high temperature expansion (HTE) of the Helmholtz free energy (HFE), up to order β^5 , of the quantum spin- S XYZ chain, with a single-ion anisotropy term and in the presence of an external magnetic field. From this result, we obtained the HTE of the classical version of the model by taking the limit $S \rightarrow \infty$. In the present paper, we apply the method of Ref. [6] directly to the classical XYZ (also with a single-ion anisotropy term and in the presence of an external magnetic field) thus simplifying enormously algebraic calculations. By this way, we are able to calculate the β -expansion of its HFE up to order β^{12} . Each coefficient of β^n in the expansion is exact ($n = -1, 0, 1, 2, \dots, 12$). Having a higher order in β allowed extending the knowledge of the thermodynamics of the classical XYZ chain up to $kT/J_x \sim 0.5$, which might be considered as an intermediate region of temperature. Joyce's exact result [2] of the classical XXZ chain, with no single-ion anisotropy term and no external magnetic field ($D = 0, h = 0$), permits knowing the behaviour of the specific heat per site at very low temperatures.

This low-temperature information can be combined with the high-temperature information by the two-point Padé approximants (PA)[11]. The best PA gives a very good description of the classical specific heat per site in the whole interval of temperature.

In the high temperature region ($J_x\beta \ll 1$), the quantum spin- S XYZ chain ($S = 1/2, 1, 3/2, 2, \dots$) is well described by the classical model. Certainly, the best application of the HFE of the classical XYZ chain is to support the study the thermodynamical properties of its quantum models for finite spin- S at lower temperatures. For $S \geq 2$ we have very few numerical analysis of the thermodynamical functions of these quantum models due to the large number of degrees of freedom to be handled. By using the Monte Carlo numerical calculation done by Yamamoto[14], for a spin-2 antiferromagnetic chain with 96 sites, we showed that its specific heat and magnetic susceptibility per site can be approximated by their respective classical results, up to $kT/J_x \approx 0.8$, within a precision of 2.5%. This gives us hope that the thermodynamics of the TMCC ($S = 5/2$) can be approximated by the HFE presented in this paper, up to this temperature, within a precision higher than 2.5%.

Finally, from the HTE for the HFE of the classical XYZ chain, which can be found in Eq.(B.1) of Appendix B, we verified that in the absence of an external magnetic field the quantum ferromagnetic and antiferromagnetic chains have the same classical limit. As a consequence of this essentially classical result, some thermodynamical functions like: mean energy, $\langle (s_i^z)^2 \rangle$, entropy and the correlation functions between first-neighbor spin components have defined parity, at $h = 0$, under the parameter transformation $(J_x, J_y, J_z) \rightarrow (-J_x, -J_y, -J_z)$. This fact permits studying the reaction of each type of chain (ferromagnetic and antiferromagnetic) to the presence of an external magnetic field.

Acknowledgments

The authors are in debt to CNPq for partial financial support. S.M. de S. and O.R. thank FAPEMIG and M.T.T. thanks FAPERJ for partial financial support.

APPENDIX A: USEFUL INTEGRALS

The normalized traces of products of operators are expressed in terms of surface integrals over unitary spheres, each of which represents the state space of a chain site. For example,

$$\langle \mathbf{H}_{1,2} \rangle \equiv \int_{S_1} d\tilde{\Omega}_1 \int_{S_2} d\tilde{\Omega}_2 \mathcal{H}(\theta_1, \phi_1, \theta_2, \phi_2), \quad (\text{A.1})$$

where the normalized solid angles $d\tilde{\Omega}_i$ are defined[16] as or

$$d\tilde{\Omega}_i \equiv \frac{\sin \theta_i}{4\pi} d\theta_i d\phi_i, \quad (\text{A.2})$$

and the function \mathcal{H} has been defined in Eq.(3). We have $\theta_i \in [0, \pi]$ and $\phi_i \in [0, 2\pi]$. Another example is

$$\begin{aligned} \langle \mathbf{H}_{1,2}^2 \mathbf{H}_{2,3} \rangle &\equiv \int_{S_1} d\tilde{\Omega}_1 \int_{S_2} d\tilde{\Omega}_2 \int_{S_3} d\tilde{\Omega}_3 \mathcal{H}(\theta_1, \phi_1, \theta_2, \phi_2)^2 \times \\ &\times \mathcal{H}(\theta_2, \phi_2, \theta_3, \phi_3). \end{aligned} \quad (\text{A.3})$$

The generalization of these formulas is straightforward. Because of the structure of the Hamiltonian (1) and the expression of spin operators (2), the integrals related to the i -th site which contribute to $H_{1,m}^{(n)}$ (see Eq. (7)), turn out to be either

$$\begin{aligned} I_\theta^{(m,n)} &\equiv \int_0^\pi d\theta (\sin \theta)^m (\cos \theta)^n \\ &= \frac{1}{4}(1 + (-1)^m)(1 + (-1)^n) \frac{\Gamma(\frac{m+1}{2})\Gamma(\frac{n+1}{2})}{\Gamma(\frac{m+n+2}{2})} \\ &\quad + \frac{1}{2}(1 - (-1)^m) \frac{(1 + (-1)^n)}{n+1} \frac{\Gamma(\frac{n+3}{2})\Gamma(\frac{m+1}{2})}{\Gamma(\frac{m+n+2}{2})}, \end{aligned} \quad (\text{A.4})$$

$$\begin{aligned} I_\phi^{(m,n)} &\equiv \int_0^{2\pi} d\phi (\sin \phi)^m (\cos \phi)^n \\ &= \frac{1}{2}(1 + (-1)^m)(1 + (-1)^n) \frac{\Gamma(\frac{m+1}{2})\Gamma(\frac{n+1}{2})}{\Gamma(\frac{m+n+2}{2})}, \end{aligned} \quad (\text{A.5})$$

where $n, m = 0, 1, 2, \dots$ and Γ is the gamma function.

APPENDIX B: THE β -EXPANSION OF THE HELMHOLTZ FREE ENERGY IN THE ABSENCE OF A MAGNETIC FIELD

The high temperature expansion of the HFE of the classical XYZ ($S \rightarrow \infty$) in the absence of an external magnetic field (Hamiltonian (1) with $h = 0$), up to order β^6 , is

$$\begin{aligned}
\mathcal{W}_{class}^{h=0} = & -\frac{\ln(2S)}{\beta} + \frac{D}{3} + \left(-\frac{J_z^2}{18} - \frac{J_y^2}{18} - \frac{J_x^2}{18} - \frac{2D^2}{45}\right)\beta \\
& + \left(-\frac{2J_y^2 D}{135} - \frac{2J_x^2 D}{135} + \frac{8D^3}{2835} + \frac{4J_z^2 D}{135}\right)\beta^2 + \left(\frac{4D^4}{14175} - \frac{32J_z^2 D^2}{4725} \right. \\
& + \frac{2J_y^2 D^2}{4725} - \frac{7J_x^4}{2700} - \frac{7J_z^4}{2700} + \frac{J_x^2 J_z^2}{225} + \frac{2J_x^2 D^2}{4725} + \frac{J_x^2 J_y^2}{225} - \frac{7J_y^4}{2700} \\
& + \left.\frac{J_y^2 J_z^2}{225}\right)\beta^3 + \left(\frac{16J_y^2 D^3}{42525} - \frac{2J_y^4 D}{2835} - \frac{32D^5}{467775} + \frac{4J_z^4 D}{2835} - \frac{2J_x^4 D}{2835} \right. \\
& + \frac{16J_x^2 D^3}{42525} + \frac{8J_x^2 J_y^2 D}{2835} - \frac{4J_y^2 J_z^2 D}{2835} + \frac{16J_z^2 D^3}{42525} - \left.\frac{4J_x^2 J_z^2 D}{2835}\right)\beta^4 \\
& + \left(-\frac{736D^6}{1915538625} - \frac{107J_x^6}{2679075} - \frac{107J_y^6}{2679075} - \frac{107J_z^6}{2679075} - \frac{844J_x^2 J_y^2 J_z^2}{893025} \right. \\
& + \frac{106J_z^4 J_x^2}{893025} + \frac{106J_z^4 J_y^2}{893025} + \frac{106J_x^4 J_y^2}{893025} + \frac{106J_x^2 J_y^4}{893025} \\
& + \frac{106J_z^2 J_y^4}{893025} + \frac{106J_z^2 J_x^4}{893025} + \frac{8768J_z^2 D^4}{49116375} + \frac{106D^2 J_x^4}{1488375} + \frac{106D^2 J_y^4}{1488375} \\
& - \frac{16J_z^4 D^2}{297675} - \frac{2008D^4 J_y^2}{49116375} - \frac{2008D^4 J_x^2}{49116375} - \frac{232J_z^2 D^2 J_x^2}{1488375} \\
& - \frac{232J_z^2 D^2 J_y^2}{1488375} + \frac{584D^2 J_x^2 J_y^2}{1488375}\Big)\beta^5 + \left(\frac{2944D^7}{1915538625} - \frac{736D^5 J_x^2}{70945875} \right. \\
& - \frac{25024J_z^2 D^5}{638512875} - \frac{736D^5 J_y^2}{70945875} - \frac{8912J_z^4 D^3}{49116375} + \frac{52D J_y^6}{1913625} + \frac{52D J_x^6}{1913625} \\
& + \frac{904D^3 J_x^4}{49116375} + \frac{904D^3 J_y^4}{49116375} - \frac{104J_z^6 D}{1913625} + \frac{6976J_z^2 D^3 J_x^2}{49116375} \\
& + \frac{6976J_z^2 D^3 J_y^2}{49116375} - \frac{4736D^3 J_x^2 J_y^2}{49116375} + \frac{52J_z^4 D J_y^2}{637875} - \frac{52J_z^2 D J_x^4}{637875} \\
& - \left.\frac{52J_z^2 D J_y^4}{637875} + \frac{52J_z^4 D J_x^2}{637875}\right)\beta^6 + \mathcal{O}(\beta^7).
\end{aligned} \tag{B.1}$$

In the absence of an external magnetic field ($h = 0$), this is an even function of the coupling constants J_x, J_y

and J_z of the Hamiltonian (1). We have confirmed this property up to order β^{12} .

-
- [1] M.E. Fisher, Am. J. of Phys. **32**, 343 (1964).
 - [2] G. S. Joyce, Phys. Rev. Lett. **19**, 581 (1967).
 - [3] H.J. Mikeska, J. Phys.: Solid St. Phys. **13**, 2913 (1980), and references therein.
 - [4] T. Delica, and H. Leschke, Physica A **168**, 768 (1990).
 - [5] O. Rojas, S. M. de Souza, E. V. Corrêa Silva, and M. T. Thomaz, Phys. Rev. B **72**, 172414 (2005).
 - [6] O. Rojas, S. M. de Souza and M. T. Thomaz, J. Math. Phys. **43**, 1390 (2002).
 - [7] O. Rojas, E. V. Corrêa Silva, W.A. Moura-Melo, S. M. de Souza, and M. T. Thomaz, Phys. Rev. B **67**, 115128 (2003).
 - [8] O. Rojas, S. M. de Souza, E. V. Corrêa Silva and M. T. Thomaz, Eur. Jour. of Phys. **B47**, 165 (2005).
 - [9] A. Büller, U. Löw, G. S. Uhrig, Phys. Rev. **B64**, 024428, (2001); B. Bernu and G. Misguich, Phys. Rev. **B63**, 134409 (2001).
 - [10] G. A. Baker Jr., G. S. Rushbrooke, H. E. Gilbert, Phys. Rev. **135**, A1272 (1964).
 - [11] G. E. Granroth, M. W. Meisel, M. Chaparala, Th. Jolicœur, B. H. Ward and D. R. Taham, Phys. Rev. Lett. **77**, 1616 (1996).
 - [12] R. J. Birgeneau, R. Dingle, M. T. Hutchings, G. Shirane and S. L. Holt, Phys. Rev. Lett. **26**, 718 (1971).
 - [13] M. T. Hutchings, G. Shirane, R. J. Birgeneau and S. L. Holt, Phys. Rev. B **5**, 1999 (1972).
 - [14] S. Yamamoto, Phys. Rev. B **53**, 3364 (1996-II); Phys. Lett. A **213**, 102 (1996).
 - [15] H.J. Jensen, O.G. Mouritsen, H.C. Fogedby, P. Hedegård and A. Svane, Phys. Rev. B **32**, 3240 (1985).
 - [16] M. Takahashi. *Thermodynamics of One-dimensional Solvable Models*. Cambridge, Cambridge University Press, 1999.

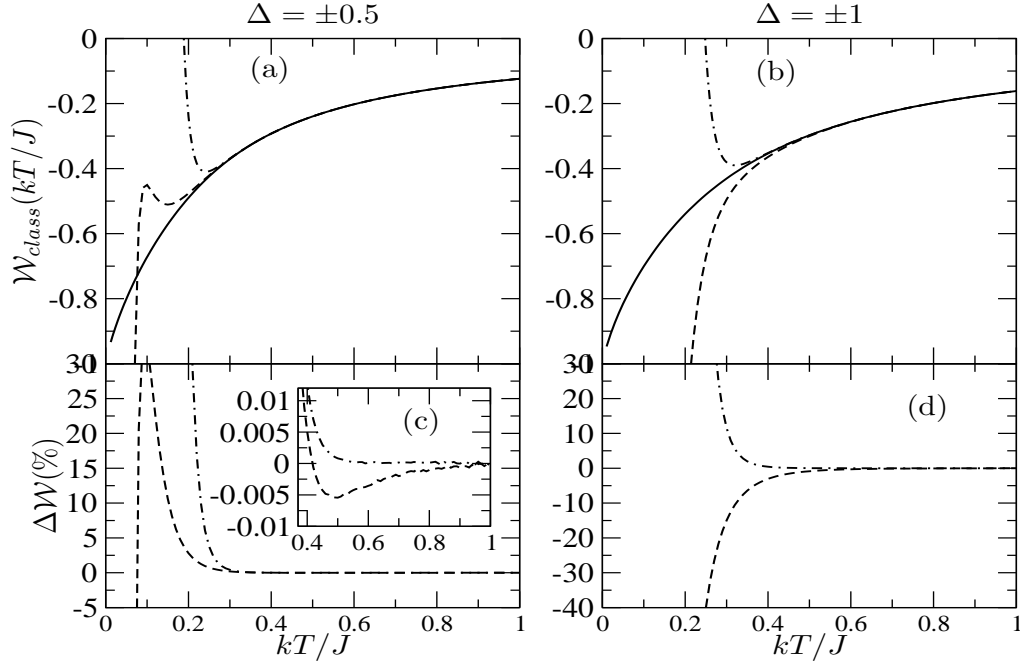


FIG. 1: (a) For $\Delta = \pm 0.5$, comparison of the numerical solution of Joyce's expression (solid line) and our HTEs up to order β^5 (dashed line) and order β^{12} (dashed-dotted line), for the HFE of the classical XXZ chain (\mathcal{W}_{class}), as a function of kT/J . In (c), the relative percent differences ($\Delta\mathcal{W}(\%)$), with respect to Joyce's exact solution, of the β^5 (dashed line) and the β^{12} (dashed-dotted line) expansions, also as functions of kT/J . In (b) and (d) a similar comparison is performed, for $\Delta = \pm 1$.

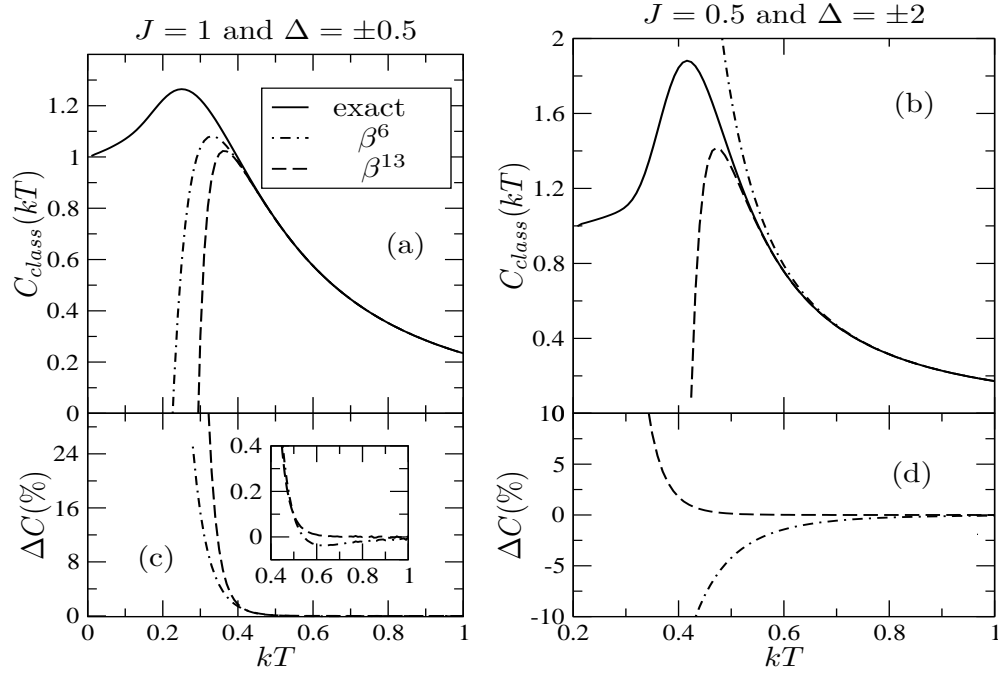


FIG. 2: (a) Specific heat per site C_{class} of the classical XXZ chain, as a function of kT , T being the absolute temperature, for $J = 1$ and $\Delta = \pm 0.5$. The upper pane shows Joyce's solution (solid line), and our expansions up to β^6 (dotted-dashed line)[5] and up to β^{13} (dashed line). The lower pane (c) shows the percent differences ($\Delta C(\%)$), with respect to Joyce's solution, of the β^6 (dotted-dashed line) and β^{13} (dashed line) expansions, also as functions of kT . Panes (b) and (d) show a similar comparison, for $J = 0.5$ and $\Delta = \pm 2$.

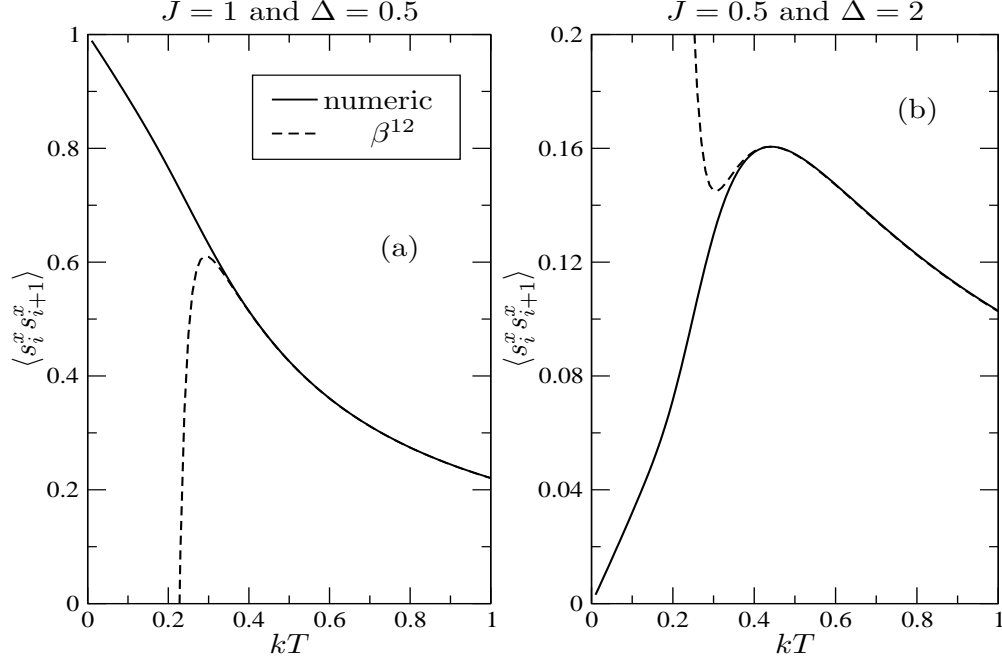


FIG. 3: The correlation function $\langle s_i^x s_{i+1}^x \rangle$ between the classical spin x -components of first neighbouring sites. The solid line stands for the exact function, whereas the dashed line stands for the HTE up to order β^{12} . In (a) we have $J = 1$ and $\Delta = 0.5$; in (b) we have $J = 0.5$ and $\Delta = 2$.

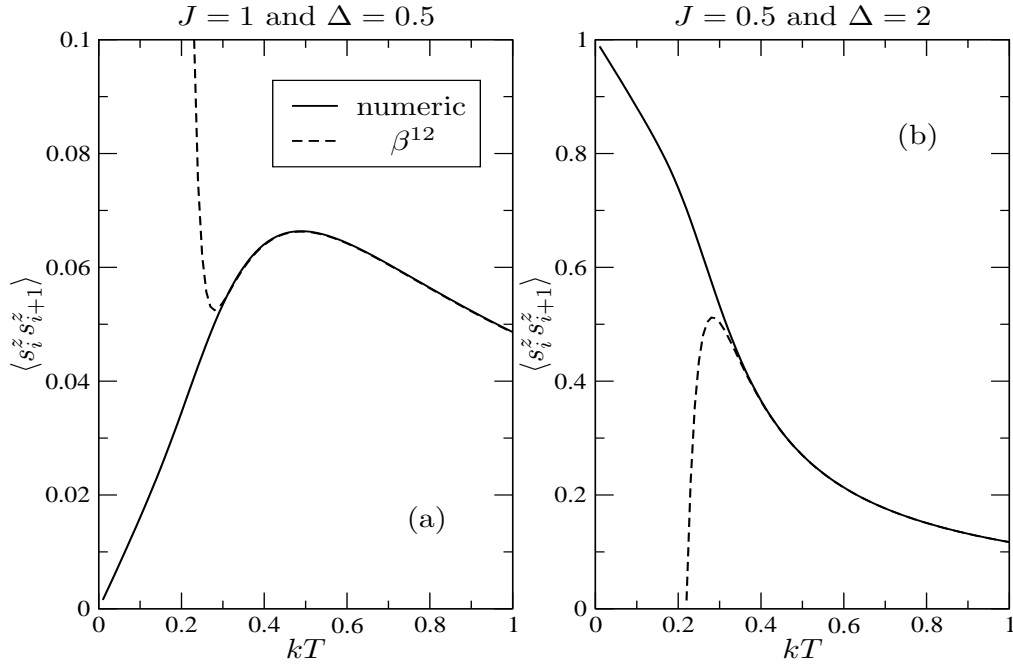


FIG. 4: The correlation function $\langle s_i^z s_{i+1}^z \rangle$ between the classical spin z -components of first neighbouring sites. The solid line stands for the exact function, whereas the dashed line stands for the HTE up to order β^{12} . In (a) we have $J = 1$ and $\Delta = 0.5$; in (b) we have $J = 0.5$ and $\Delta = 2$.

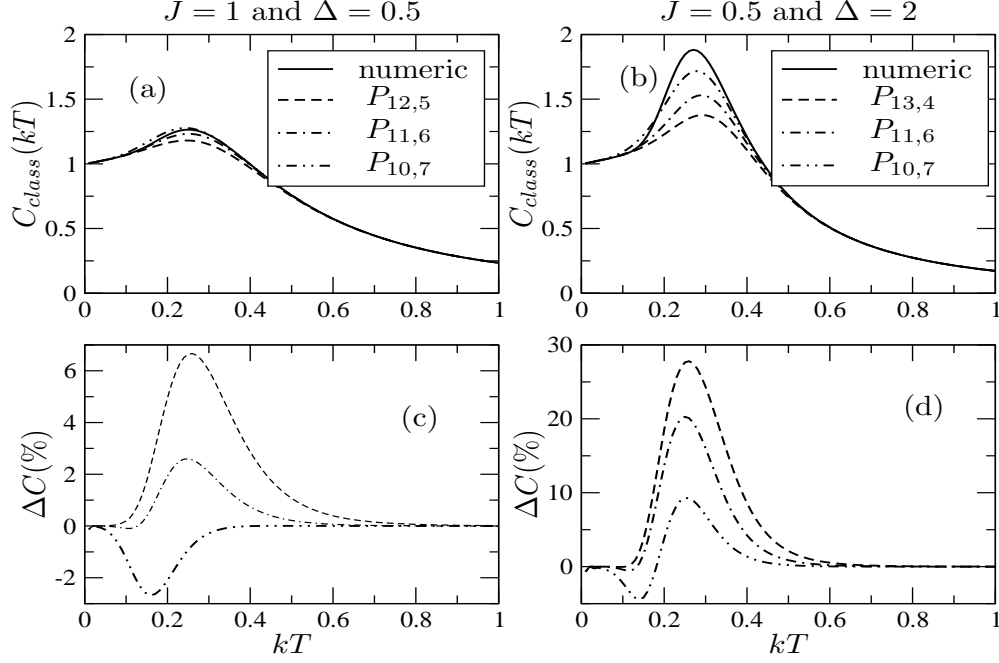


FIG. 5: Upper panes (a) and (b) compare exact classical specific heat per site and their best PAs. Lower panes (c) and (d) show the percentual difference of each PA with respect to the exact result. In (a) and (c) we have $J = 1$ and $\Delta = 0.5$, whereas in (b) and (d) we have $J = 0.5$ and $\Delta = 2$.

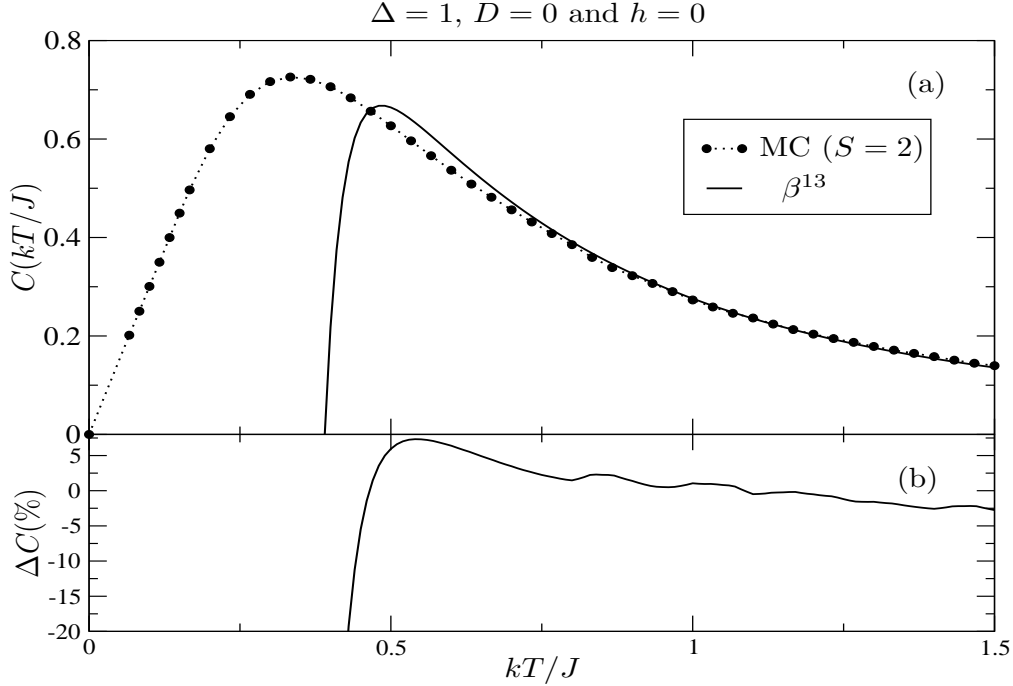


FIG. 6: (a) The dots correspond to the Monte Carlo (MC) calculation of the specific heat per site for the $S = 2$ antiferromagnetic chain[14], for $D = 0$ and $h = 0$, as a function of kT , where T is the absolute temperature. The solid line corresponds to our HTE of the classical specific heat up to order β^{13} . (b) The relative percentual difference of the two curves.

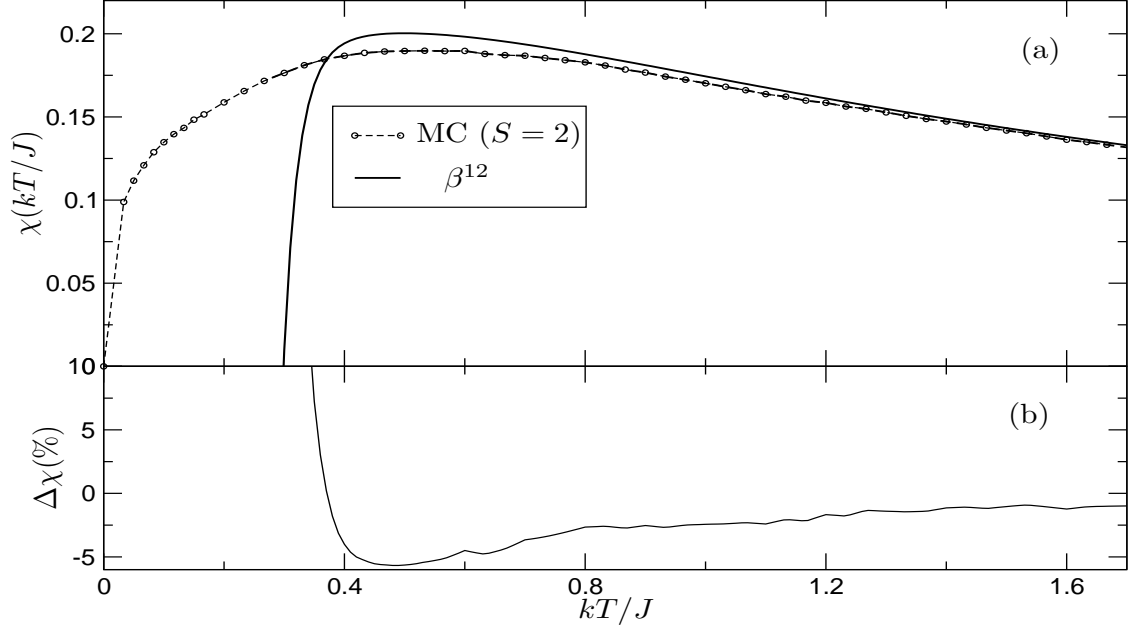


FIG. 7: In (a) we compare Yamamoto's MC calculation of the magnetic susceptibility per site of the $S = 2$ antiferromagnetic chain[14] (dots and dashed line) and the HTE of its classical equivalent, up to order β^{12} (solid line). In (b), we have the percental difference of the two functions plotted in (a). We have $\Delta = 1$, $D = 0$ and $h = 0$.

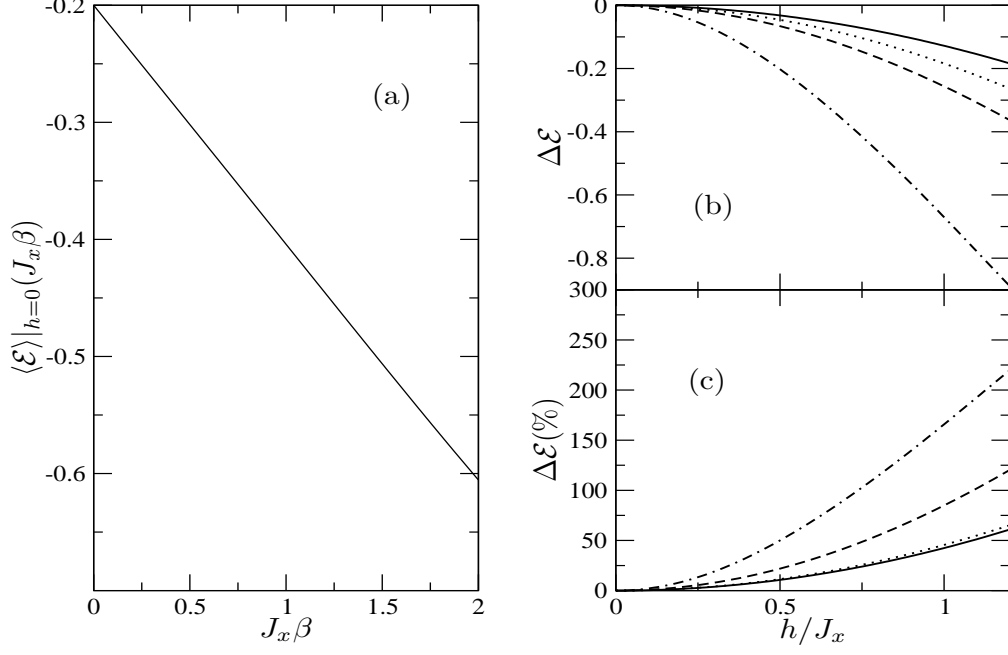


FIG. 8: (a) The mean energy per site $\langle \mathcal{E} \rangle$ of ferromagnetic ($J_z/J_x = -2/3$) and antiferromagnetic ($J_z/J_x = 2/3$) media in the absence of an external magnetic field. (b) The difference $\Delta \mathcal{E}$ of the mean energy per site at finite h and its value at $h = 0$ versus h/J_x . We plot the antiferromagnetic case for $J_x \beta = 0.5$ (solid line) and $J_x \beta = 1$ (dotted line); and also the ferromagnetic case for $J_x \beta = 0.5$ (dashed line) and $J_x \beta = 1$ (dotted-dashed line). In (c) we have the correspondent percentual differences $\Delta \mathcal{E}(\%)$ with respect to the $h = 0$ case; the same graphical convention for lines is used. In all figures we have $J_y/J_x = 1/3$ and $D/J_x = -0.6$.

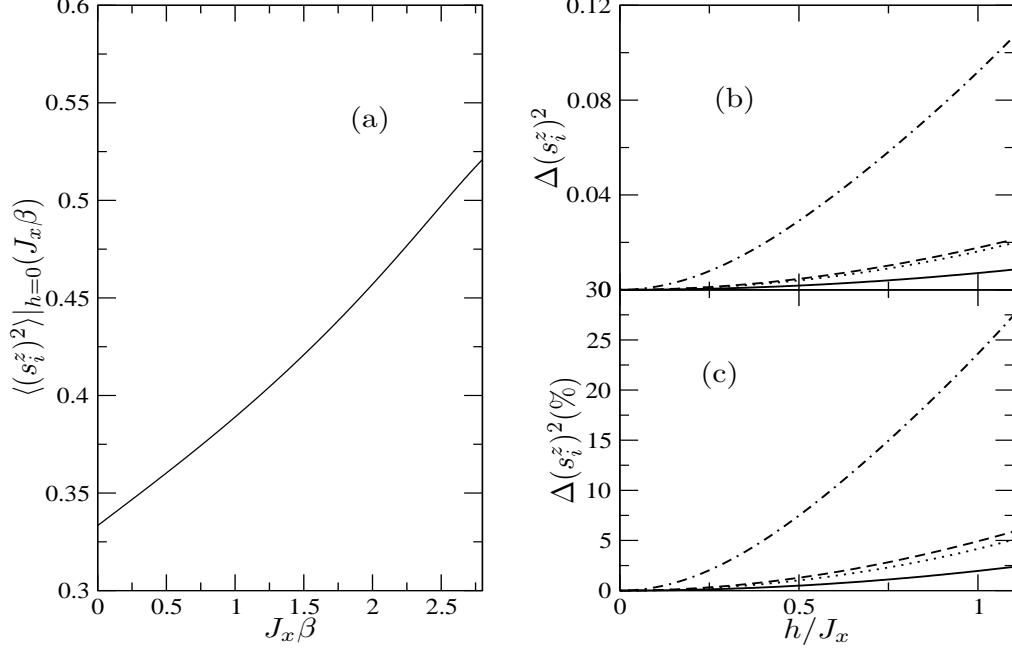


FIG. 9: (a) The mean value of the squared z -component of spin per site $\langle (s_i^z)^2 \rangle$ for ferromagnetic ($J_z/J_x = -2/3$) and antiferromagnetic ($J_z/J_x = 2/3$) media is the same, in the absence of an external magnetic field. (b) The difference of $\langle (s_i^z)^2 \rangle$ at finite h and its value at $h = 0$ versus h/J_x . We plot the antiferromagnetic case at $J_x\beta = 0.5$ (solid line) and $J_x\beta = 1$ (dotted line); and the ferromagnetic case at $J_x\beta = 0.5$ (dashed line) and $J_x\beta = 1$ (dotted-dashed line). Fig. (c) shows the corresponding percentual differences with respect to the $h = 0$ case; the same graphical convention for lines is used. In all figures we have $J_y/J_x = 1/3$ and $D/J_x = -0.6$.

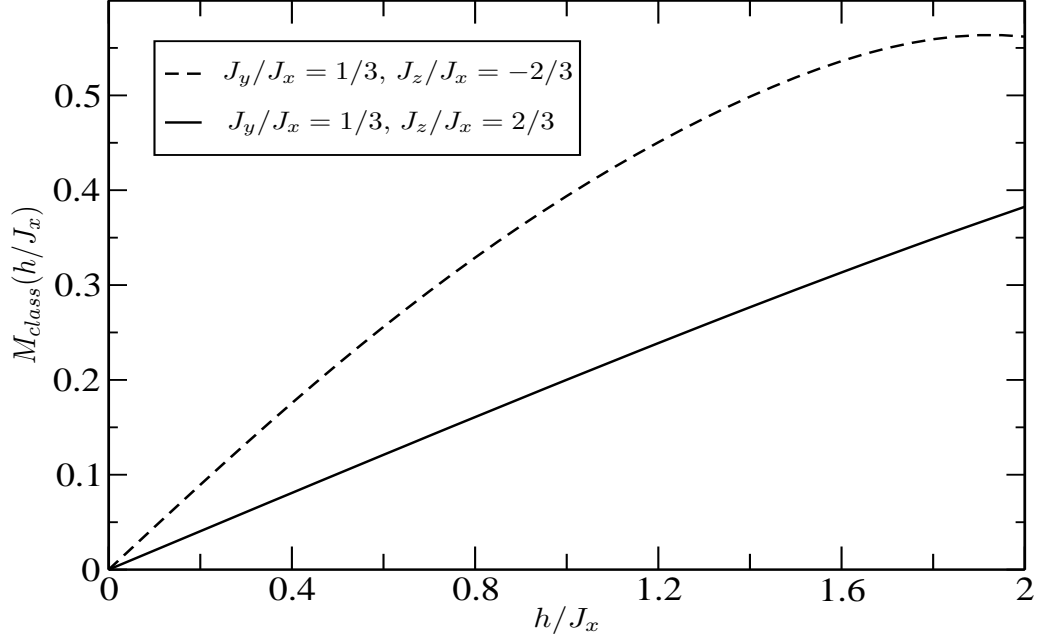


FIG. 10: The classical magnetization per site M_{class} as a function of h/J_x with $J_y/J_x = 1/3$ and $D/J_x = -0.6$ at $J_x\beta = 0.8$, for the ferromagnetic ($J_z/J_x = -2/3$, dashed line) and antiferromagnetic ($J_z/J_x = 2/3$, solid line) cases.

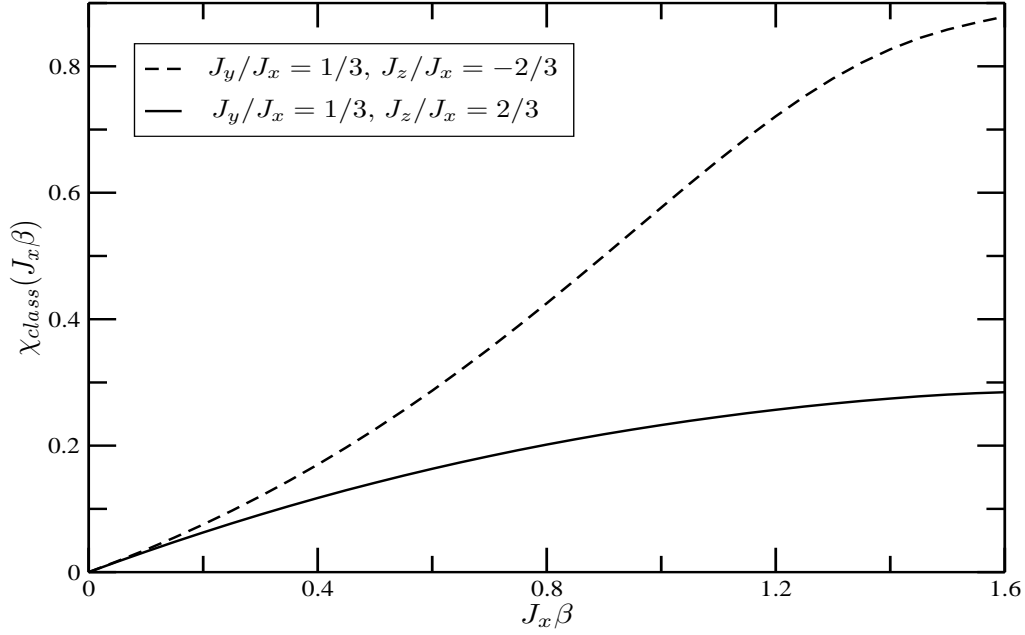


FIG. 11: The classical magnetic susceptibility per site χ_{class} as a function of $J_x\beta$ with $J_y/J_x = 1/3$ and $D/J_x = -0.6$ at $h/J_x = 0.35$, for the ferromagnetic ($J_z/J_x = -2/3$, dashed line) and antiferromagnetic ($J_z/J_x = 2/3$, solid line) cases.

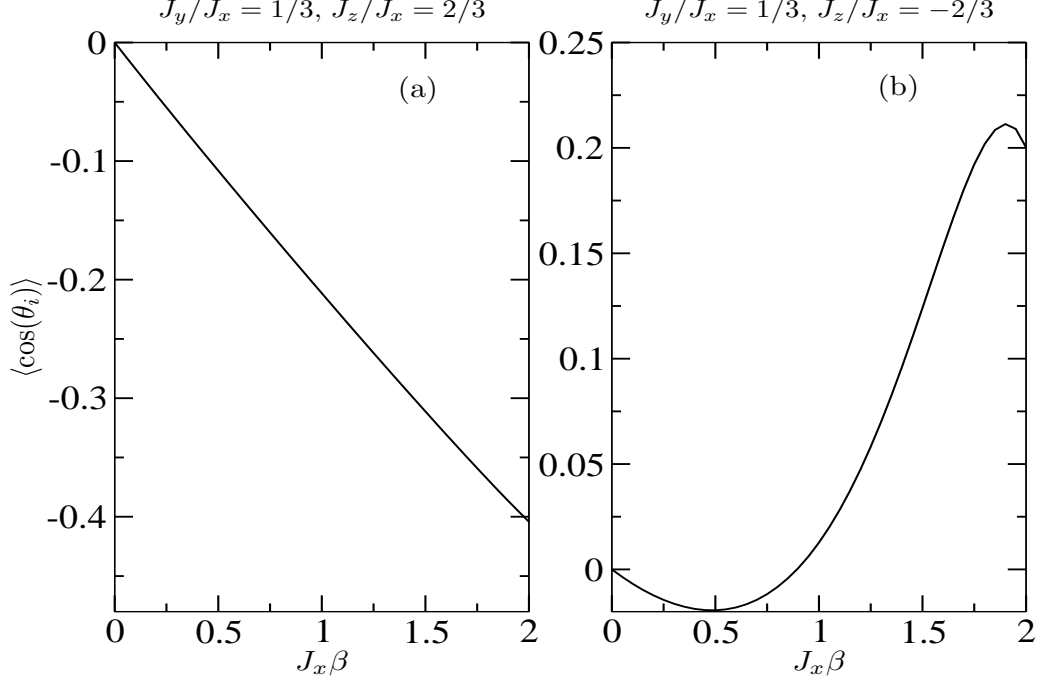


FIG. 12: The function $\langle \cos \theta_i \rangle$ as a function of $J_x\beta$, for $i = 1, 2, \dots, N$ with $J_y/J_x = 1/3$ and $D/J_x = -0.6$ at $h/J_x = 0.35$. Fig. (a) shows the antiferromagnetic case ($J_z/J_x = 2/3$) and Fig. (b) the ferromagnetic case ($J_z/J_x = -2/3$).

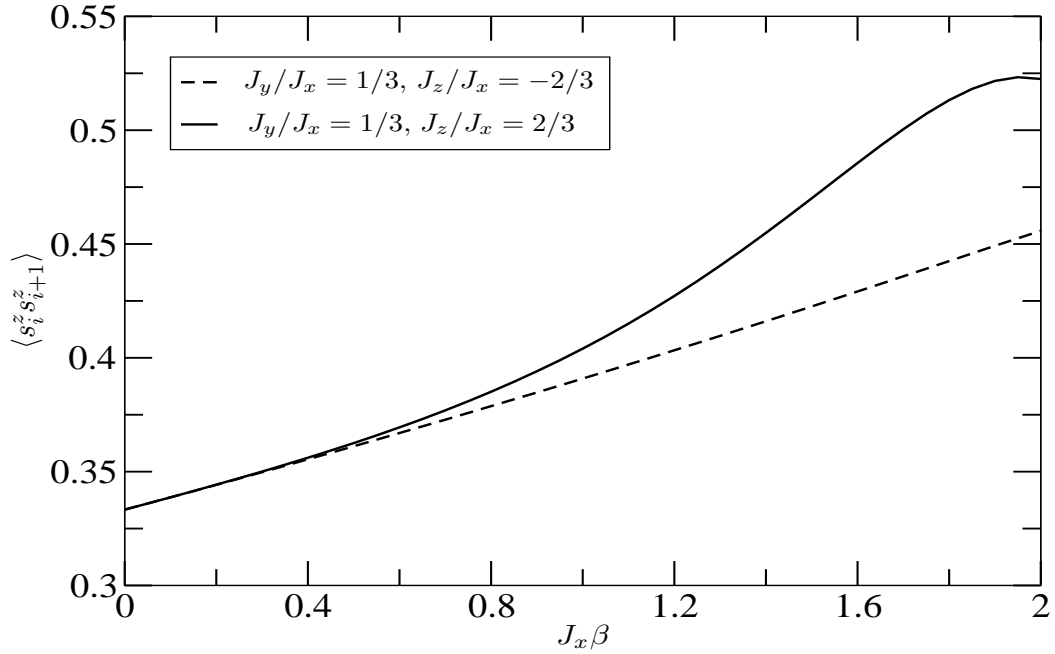


FIG. 13: The correlation function $\langle s_i^z s_{i+1}^z \rangle$ between the spin z -components of first neighbors as a function of $J_x\beta$. The dashed and solid lines describe the ferromagnetic case ($J_z/J_x = -2/3$) and antiferromagnetic case ($J_z/J_x = 2/3$), respectively. We take $J_y/J_x = 1/3$ and $D/J_x = -0.6$ at $h/J_x = 0.35$.